Chemical Engineering Journal 110 (2005) 11–18

Chemical Engineering Journal

www.elsevier.com/locate/cej

Axial dispersion in single pellet-string columns packed with unusually shaped porous pellets

Olga Šolcová *, Karel Soukup, Petr Schneider

Institute of Chemical Process Fundamentals, Czech Academy of Sciences, 16502 Praha 6, Czech Republic

Received 21 May 2004; accepted 26 January 2005

Abstract

Axial dispersion in the single pellet-string arrangement of a chromatographic column (SPSC) packed with 15 types of pellets with various shapes was studied. Non-porous cylindrical pellets and non-spherical porous pellets with pores blocked by a liquid (Porofil) were used. For different tracer- and carrier-gases (carrier-gases: N_2, H_2; tracer-gases: H_2, He, N_2, Ar) comparable dependencies of Bodenstein numbers, *Bo*, versus the product of Reynolds and Schmidt numbers, *Re Sc*, were obtained. Tracer dispersion due to extra-column effects was eliminated via convolution of column responses for two column lengths. Reproducibility of axial dispersion determination was verified by repeated column repacking. An interpolation equation for different pellet shapes was proposed. The pellet shape is characterized through pellet sphericity, φ, and the pellet/column diameter ratio, d_p/d_c. The effectiveness of axial dispersion correlations was confirmed for sphericity 0.427–0.89 and the pellet/column diameter ratios 0.35–0.87.

Keywords: Dispersion; Mass transfer; Parameter identification; Particle; Single pellet-string column; Axial dispersion

1. Introduction

Knowledge of effective diffusion coefficients and other transport characteristics that affect rates of steps inside the porous materials is indispensable for modern engineering design of chemical and biochemical processes. Therefore, an effort to improve the accuracy of effective diffusion coefficients and/or transport parameters obtained by a number of methods is seen [1–4].

One of the well-established techniques [5,6] is the chromatographic approach that permits to study diffusion under dynamic condition. Porous particles can be packed in the column in two ways: a wide column packed with particles; the column to particle diameter ratio should be large enough, say about 1:20, to satisfy conditions for axially dispersed plug-flow, or, particles are packed one-by-one into a column with diameter that is only slightly larger than the particle diameter (this arrangement is known as single pellet-string column (SPSC [7])). The advantage of the SPSC method is that whole pellets in their original shape can be used. The simplicity of the equipment as well as the speed of data acquisition is the main reasons for the frequent use of this technique. Recently, Li et al. [8] used SPSC to obtain effective diffusion coefficient and tortuosity factor of ammonia synthesis catalyst; similarly Costa and Rodrigues [9] determined intraparticle mass transport parameters by chromatographic method with a single pellet-string fixed bed. SPSC arrangement was also utilized by Li et al. [10], Colaris et al. [11] and Yu et al. [12] for determination of intraparticle diffusivity.

Effective diffusivities are evaluated from response curves of columns packed with the tested porous materials (chromatographic peaks). A pulse of tracer-gas (T) is injected into the carrier-gas (C) that flows through the column at constant flow-rate. Tracer concentration is monitored at the column outlet. Model of processes in the column due to Kubín [13] and Kučera [14] is nearly exclusively used for the analysis of outlet peak. This model neglects extra-column effects (the effects of processes upstream and downstream of the column).

* Corresponding author. Tel.: +420 220 390 279; fax: +420 220 920 661.
E-mail address: solcova@icpf.cas.cz (O. Šolcová).

1385-8947/$ – see front matter © 2005 Elsevier B.V. All rights reserved.
doi:10.1016/j.cej.2005.01.010

The inclusion of these processes into the time-domain peak matching via the application of the convolution theorem was shown by Šolcová and Schneider [15]. This requires, besides the knowledge of the experimental system response, also the separate knowledge of extra-column responses, or experimental system responses for two different column lengths.

In general this approach requires simultaneous search for quite a number of parameters (in addition to the tracer-gas residence time and tracer axial dispersion, the tracer transport through the laminar film around packing particles, tracer diffusion in the packing pore structure and adsorption rate and equilibrium on the pore surface). To prevent adsorption and the possible surface diffusion, which obscure the effective diffusion coefficients, it is possible to employ non-adsorbable carrier- and tracer-gases and to work with higher carrier-gas velocities. Then, only parameters for tracer residence time in the interparticle space (t_c), tracer axial dispersion (Pe) and pore-diffusion time (t_{dif}), which contains the effective diffusion coefficient of the pair T–C (D_{TC}), need to be fitted. Unfortunately, the tracer axial dispersion and the pore-diffusion parameters are highly correlated, which makes the obtained effective diffusion coefficients much less confident.

We suggested [16] the possibility to determine the tracer axial dispersion independently by the use of non-porous (e.g. metallic) pellets of the same shape as the porous pellets in question. The axial dispersion coefficients lump together all mechanisms leading to axial mixing in packed beds. Thus, the axial dispersion coefficient must account not only for molecular diffusion and convective mixing but also for non-uniformities in the fluid velocity across the packed bed. It was confirmed that Peclet numbers for identical carrier- and tracer-gases and carrier flow-rates are the same for columns packed with non-porous and porous particles of the same shape. If non-porous packing is used, then, only two parameters appear in the theoretical impulse response: Pe and t_c. Their determination by time-domain matching is rapid and parameters are uncorrelated. The use of separately determined Peclet numbers decreases the number of matched parameters for porous packing and therefore significantly improves the confidence of obtained pore-diffusion characteristics. Based on the Edwards and Richardson [17] empirical equation, we have suggested an interpolation equation that was verified for spherical and cylindrical pellets. Recently, a new generation of porous catalysts or adsorbents has appeared in chemical industry that has higher outer surface to volume ratios. These pellets have non-standard shapes, e.g. asterisks, lumps, irregular spheres, cylindrical extrudates, trilobes, etc. For such pellets shapes it is nearly impossible to set-up the non-porous (metal) twins.

It is the aim of this work to develop interpolation equations for axial dispersion for a wide range of non-standard pellet shapes and sizes.

First it was necessary to develop a method for obtaining non-porous twins of unusually shaped porous pellets that could be used for independent determined of axial dispersion characteristics. We have tried to fill all pores in porous pellets by a suitable liquid that blocks the access for tracer- and carrier-gases and, thus, to remove the intraparticle pore-diffusion process. In this way, the soaked-up pellets should behave as non-porous.

2. Experimental

2.1. Used materials

Eight industrial and one laboratory prepared porous pellets with various shapes and sizes and brass cylindrical pellets were chosen for testing. Sizes of non-porous cylindrical pellets (height H and diameter D) are summarized in Table 1. Shapes of used porous pellets are shown in Fig. 1 and their textural properties are summarized in Table 2. Textural properties of porous pellets were determined by mercury porosimetry, helium pycnometry and physical adsorption of nitrogen (AutoPore III, AccuPyc 1330 and ASAP2010M, Micromeritics, USA). All tested pellets fulfilled the basic condition of SPSC arrangement that two pellets may not be packed alongside each other.

2.2. Image analysis

Volume and outer surface area of irregularly shaped pellets (required for sphericity evaluation) were determined by image analysis from bitmap pictures of porous materials obtained by Canon scanner (CanonScan Lide 30). Resolution of 1200 DPI was sufficient for determination of detailed shapes of pellets (see Fig. 1). For image analysis the SigmaScanPro (SPSS Inc., USA) software was used.

Table 1
Non-porous cylindrical pellets

Pellet	Diameter, D (mm)	Height, H (mm)
Cyl 0.78	4.00	3.10
Cyl 1.02	4.07	4.17
Cyl 1.1	4.05	4.45
Cyl 1	4.40	4.40
Cyl 1.5	4.00	6.00
Cyl 0.98	4.90	4.80

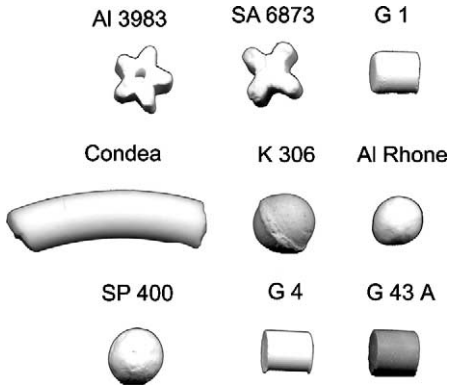

Fig. 1. Shapes of porous pellets.

Table 2
Textural properties of porous pellets

Pellet code[a]	Manufacturer	Porosity (%)	S_{BET} (m^2/g)	Most frequent pore radii[b] (nm)
Al 3983	Süd-Chemie AG, Germany	0.55	6.0	42, 430
SA 6873	Norton, England	0.64	213.7	2, 190
G1	Laboratory prepared from boehmite[c]	0.58	3.4	46, 2330
G4	Laboratory prepared from boehmite[c]	0.52	5.8	46, 630
G43A	Süd-Chemie AG, Germany	0.60	183	3.5, 254
SP 400	Alcoa, USA	0.57	277	2.1, 38, 100, 260
Al-RHONE	Kaučuk Kralupy, Czech Republic	0.66	188	120
K306	Süd-Chemie AG, Germany	0,53	136.5	2.5, 50
CONDEA	Chemopetrol, Litvínov, Czech Republic	0.62	85	2.5

[a] For pellet shapes, see Fig. 1.
[b] From mercury porosimetry.
[c] For preparation procedure, see [20].

2.3. Single pellet-string columns

Stainless steel columns with two internal diameters (7 mm and 8 mm) were used. To remove the extra-column effects by convolution it was necessary to obtain experimental system responses for two lengths of each column. The length of the shorter column (denoted as I) was $L_I = 50$ cm and of the longer column (II) $L_{II} = 100$ cm. Non-porous pellets or pellets with liquid blocked pores were packed randomly one-by-one into column of both lengths (see Fig. 2). Table 3 shows the geometric properties of pellets and packed columns; pellet equivalent sphere diameters (d_p, diameter of a sphere with the same ratio of outer surface and volume as the pellet), pellet sphericities, pellet/column diameter ratios (d_p/d_c), for cylindrical pellets also height/diameter ratios (H/D) and the corresponding packed column void fractions, α. The sphericity, φ, defined as the ratio of the surface area of the sphere of the same volume as the particle and the surface area of particle was used to enable characterizing of more complicated particle geometries. Thus, for spherical particles $\varphi = 1$ and for cylindrical pellet $\varphi_{cylinder}$ is given as: $[18(H/D)^2/(1 + 2(H/D)^3)]^{1/3}$, where H/D is the cylindrical pellet height, H, to diameter, D, ratio (e.g. for any $H/D = 1$, $\varphi = 0.874$).

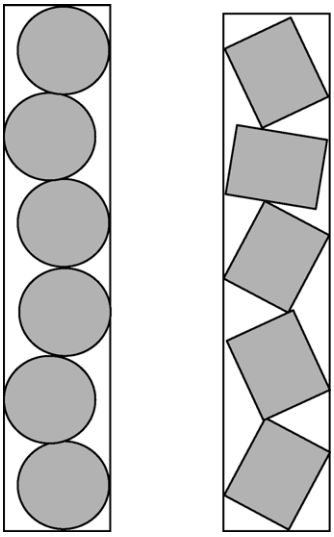

Fig. 2. Packing of spherical and cylindrical pellets in the SPSC arrangement.

The basic condition of SPSC arrangement is that for *spherical pellets* $d_p/d_c > 1/2$, hence, two pellets are never packed alongside each other. This condition was valid for all pellets used including asterisk pellets AL3983 and SA 6873 that, due to the low sphericities, have very low d_p (2.45 and 3.04 mm, respectively).

2.4. Gases

Nitrogen and hydrogen were used as carrier-gases (C). Hydrogen, helium, argon and nitrogen were used as tracer-gases (T).

2.5. Liquid

The fluorinated hydrocarbon Porofil 3 (Beckman-Coulter, USA) was used for pore blocking. According to the manufacturer $\sigma \cos\theta = 0.16$ bar μm (where σ is the surface tension, and θ the contact angle). From comparison of capillary outflow-time for water and Porofil its viscosity was estimated as $\mu = 1.25$ mPa s.

2.6. Pore blocking

To guarantee blocking of all pores by Porofil, porous pellets were at first evacuated at 200 Pa for 10 min and under vacuum submerged into Porofil. After 45 min the excess of Porofil was decanted and the drops of Porofil from their outside surface were removed.

Chromatographic system consisted of a calibrated mass flow-meter-controllers for carrier- and tracer-gases (Brooks model 5850S, Brooks Instrument, The Netherlands), a six-way sampling valve for tracer-gas with sampling loop 0.273 cm^3, single pellet-string column and a thermal conductivity detector (Micro-TCD 10-955; Gow-Mac Instruments Co., England; cell volume 20 μl). Metal capillaries (i.d. 1 mm) with minimized length were employed for connecting the system components.

Table 3
Geometric properties of non-spherical pellets and packed columns

Pellets code/porosity	d_p (mm)	d_p/d_c	Sphericity, φ	Height/diameter of pellets, H/D[a]	Column void fraction, α
Al 3983/porous	2.45	0.35	0.427		0.642
SA 6873/porous	3.04	0.38	0.535		0.710[b]
Cyl 0.78/non-porous	3.64	0.52	0.867	0.78	0.674
G1/porous	4.12	0.59	0.874	1.01	0.640
Cyl 1.02/non-porous	4.13	0.59	0.874	1.02	0.641
G4/porous	4.18	0.60	0.873	1.02	0.644
Cyl 1.1/non-porous	4.27	0.61	0.873	1.10	0.650
G43A/porous	4.40	0.63	0.874	1.00	0.600
Cyl 1/non-porous	4.40	0.63	0.874	1.00	0.601
Cyl 1.5/non-porous	4.48	0.64	0.859	1.50	0.574
Cyl 0.98/non-porous	4.83	0.69	0.874	0.98	0.515
SP 400/porous	5.30	0.74	0.890		0.617
Al-RHONE/porous	5.89	0.76	0.830		0.664
K306/porous	5.70	0.81	0.770		0.572
CONDEA/porous	6.12	0.87	0.735	3.96	0.616

[a] For cylinders only.
[b] 8 mm (i.d.); others 7 mm (i.d.).

3. Column responses

All measurements were performed at laboratory temperature and pressure. The maximum pressure drop across the column was always less than 500 Pa and, therefore, neglected. At least three responses were obtained for every pair of tracer- and carrier-gas and each carrier-gas flow-rate. For all experiments the same sampling loop was used to introduce the tracer-gas impulse. Hence, the injected amount of tracer-gas was always the same. Injection of tracer T into carrier C is denoted in the following as T → C. Usually 1000 signal points from the TCD were logged into computer.

3.1. Signal processing

After zero-line correction (less than 0.1% of the maximum response height) the signal was reduced to approximately 100 uniformly distributed points and normalized by the maximum tracer concentration.

To remove possible fluctuations due to tracer injection and start of data logging the replicated peaks were shifted to the mean of maxima positions. The positions of peak maxima differed only slightly (between 0.1 and 0.2 s). When the difference was higher the peaks set measurements was repeated. The final response peak was, then, obtained by averaging the individual responses in the set.

3.2. Evaluation of column responses

For a T → C system the impulse response (i.e. response to a tracer Dirac pulse) of a column packed with non-porous spherical particles is given e.g. by Himmelblau and Bischoff [18],

$$h(t) = \frac{1}{t_c}\sqrt{\frac{Pe\, t_c}{4\pi t}} \exp\left[-\frac{Pe\, t_c}{4t}\left(1-\frac{t}{t_c}\right)^2\right] \quad (1)$$

where t_c is the tracer mean residence time in the column of length L_c ($t_c = L_c/v$) with carrier-gas *interstitial linear* velocity, v. *Pe* the Peclet number ($Pe = vL_c/E_{TC}$ and E_{TC} the axial dispersion coefficient for the pair *T–C*, defined per unit free cross section of the column). Eq. (1) is based on simplified assumptions of axially dispersed plug-flow and pseudo-homogeneous column packing; the true situation is, of course, much more complicated and hardly tractable.

Responses for two column lengths, II and I ($L_{II} > L_I$) were used together with the convolution theorem to remove the extra-column effects (due to, i.e., connection tubing, sampling valve, thermal conductivity detector, column inlet and outlet, etc.). The column response from the longer column II (length L_{II}), $c(t)$, is given by

$$c(t) = \int_0^t g(t-u)h(u)\,\mathrm{d}u \quad (2)$$

where $g(t)$ describes the shape of the signal entering to the column instead of the Dirac pulse (in our case the experimental response for the shorter column I (length L_I), was used). Then $h(t)$ is the impulse response for a column of length $L_c = L_{II} - L_I$. The method is in detail described elsewhere [15].

The integrals (2) were evaluated numerically and simplex algorithm was used for searching of optimum t_c and *Pe* parameters corresponding to column length $L_c = L_{II} - L_I$. The minimized objective function was the sum of squared deviations between experimental and calculated responses of column II. All used numerical algorithms were taken from Press et al. [19]; for details, see [16].

The tracer residence time, t_c, was also obtained independently from the known carrier-gas volumetric flow-rate, column void fraction and column volume (corresponding to column length $L_{II} - L_I$). In all cases the agreement was excellent.

The information on axial dispersion is contained in the Peclet numbers, *Pe*. In order to abstract the column length,

Table 4
Binary bulk-diffusion coefficients [21]

Gas pair	$\mathbf{D}^{m}_{TC}$ (298 K, 101.325 kPa) (cm^2/s)
N_2–Ar	0.199
N_2–He	0.712
H_2–He	0.748
N_2–H_2	0.789
H_2–Ar	0.818

L_c, from *Pe* we have used Bodenstein numbers, *Bo*, which use the packing particle size as the characteristic dimension. For spherical pellets the sphere diameter and for other pellet shapes the equivalent sphere diameter, d_p, was used: $Bo = vd_p/E_{TC}$. Hence $Bo = Pe(d_p/L_c)$.

The product of Reynolds and Schmidt numbers, $Re\,Sc = vd_p/\mathbf{D}^{m}_{TC}$ (for the binary bulk gas diffusivity, $\mathbf{D}^{m}_{TC}$, see Table 4), were used as the measure of carrier-gas velocity and type. The linear interstitial carrier-gas velocity, v, was obtained from the fitted t_c parameter.

4. Results and discussion

4.1. SPSC reproducibility

It was shown previously [16] that if pellets are placed into the column one-by-one, quite regular and reproducible column packing is obtained. This was confirmed not only for non-porous spherical pellets with $d_p > d_c/2$, but also for non-porous cylindrical pellets with different ratios of height and diameter, *H*/*D*. The relative standard error of column void fraction, α, obtained from several-fold columns repacking amounted to 0.6%. For pellets with pores blocked by Porofil similar repacking resulted in 0.4% standard error. For pellets G43A, the number of pellets repacked into columns of both lengths I and II was the same (115 for 0.5 m column I and 230 for 1 m column II) and for Al 3983 pellets the number of repacked pellets differed only by one (79 or 80 for 0.5 m column I and 160 or 161 for 1 m column II). The obtained standard error resulted from differences between volumes of individual pellets.

4.2. Extra-column effects

The magnitude of extra-column effects is illustrated in Fig. 3, which shows column responses for both column lengths and the same carrier-gas flow-rate (peaks 2 and 3). The calculated impulse response, which corresponds to the shorter column I (peak 1) is also shown. As the difference between lengths of columns II and I, $L_{II} - L_I$, is the same as the length of the shorter column I, L_I, the difference between peak 1 (impulse response) and peak 2 (shorter column) shows the influence of extra-column effects. Peclet numbers calculated directly from the shorter column response (i.e. neglecting extra-column effects) differ up to 10–20% from the correct value (when signal convolution is applied).

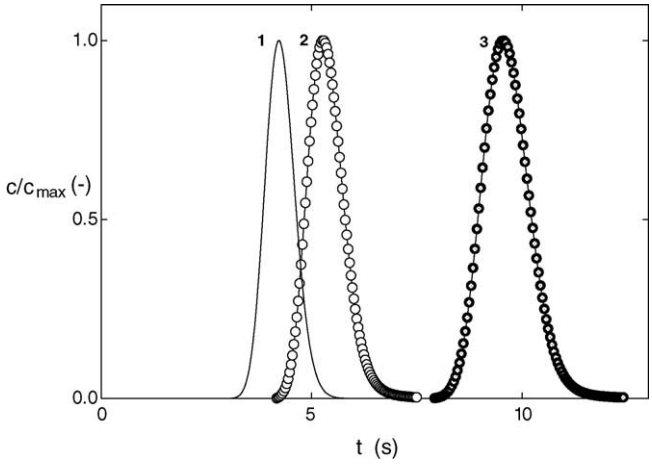

Fig. 3. H_2 (tracer) → N_2 (carrier) peaks for SA 6873 pellets with $d_p/d_c = 0.38$ and sphericity $\varphi = 0.535$ and nitrogen flow-rate 250 cm^3/min ($v = 11.7$ cm/s, $Re\,Sc = 4.57$). Column responses: (3) long column ($L_{II} = 100$ cm), (2) short column ($L_I = 50$ cm); (1) impulse response for column of length $L_c = L_{II} - L_I = 50$ cm. Points: experimental; lines: calculated. Fitted parameters: $t_c = 4.2$, $Pe = 297$ ($Bo = 1.8$).

4.3. Pore blocking

Two types of porous pellets (G43A, G1) with pores blocked by Porofil and non-porous brass pellets (Cyl 1, Cyl 1.02) of the same shape (see Table 3) were chosen for comparison of axial dispersion coefficients. In Fig. 4 the axial dispersion coefficients (in the form of *Bo* numbers) obtained for different pairs of tracer-carrier-gases and velocities ($Re\,Sc \in (1–50)$) are shown. *Bo* numbers for porous pellets with blocked pores and non-porous pellets with the same shape are nearly identical in the whole range of *Re Sc*. It can be seen that the spread of *Bo* numbers for both packing types are similar to the ordinary *Bo* reproducibility. It can be concluded that Porofil blocked all pores in porous particles and filled porous particles behaved as non-porous.

4.4. Axial dispersion reproducibility

The reproducibility of the axial dispersion determination can be judged by comparing results for repeatedly repacked

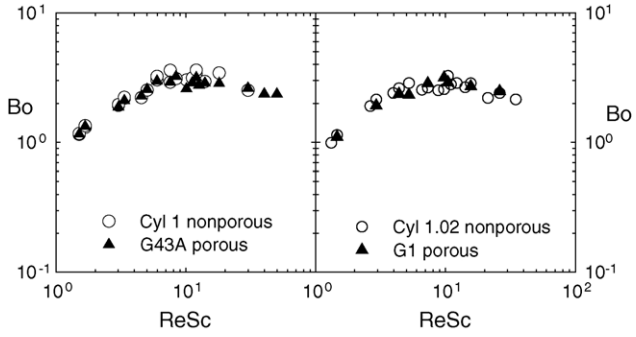

Fig. 4. *Bo*–*Re Sc* dependences for different tracer-gases and porous pellets (G43A, G1) with pores blocked by Porofil and non-porous brass pellets (Cyl 1, Cyl 1.02) with identical shapes (see Table 3).

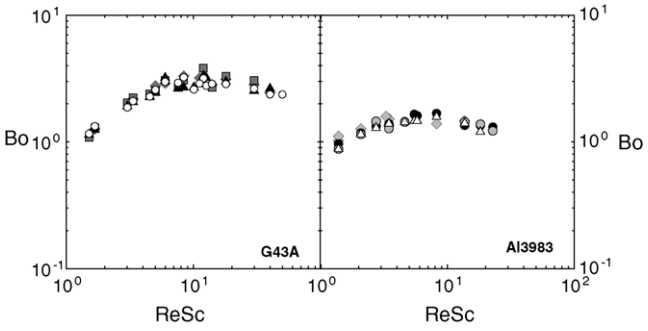

Fig. 5. Reproducibility of *Bo–Re Sc* dependences for four-fold repacking of cylindrical pellets G43A and three-fold repacking of asterisk pellets Al 3983.

columns of with cylindrical pellets G43A (four-fold repacking) and with asterisk shaped pellets Al 3983 (asterisks with a central hole; three-fold repacking). In Fig. 5 the *Bo–Re Sc* dependence is shown for both pellet shapes. It is seen that Bo from repeated measurements are consistent. This is true for quite a wide range of sphericity (φ(Al 3983) = 0.427, φ(G43A) = 0.874).

Table 5
Parameters of correlation equations (3) and (4)

Parameter	Non-spherical pellets	Spherical pellets
γ	1.117	1.087
λ_0	0.666	9.963
λ_1	0.764	1.18
λ_2	4.629	–
β	16.163	81.47

4.5. Correlation of axial dispersion

Fig. 6 summarizes the obtained axial dispersion characteristics for pellets of 15 types (6 types of non-porous cylindrical pellets and 9 types of non-spherical porous pellets with pores blocked by Porofil) in the form of Bo versus *Re Sc*. For data correlation the empirical interpolation equation (3) was applied. *Bo* is correlated with the dimensionless product *Re Sc*; the pellet shape is taken into account through two parameters: the ratio of equivalent sphere diameter and column diameter, d_p/d_c, and pellet sphericity, φ. Five adjustable parameters (β, γ, λ_0, λ_1, λ_2) obtained by non-linear fitting are summarized in Table 5. This equation is an extension of the Edwards and Richardson equation [17] and our recent

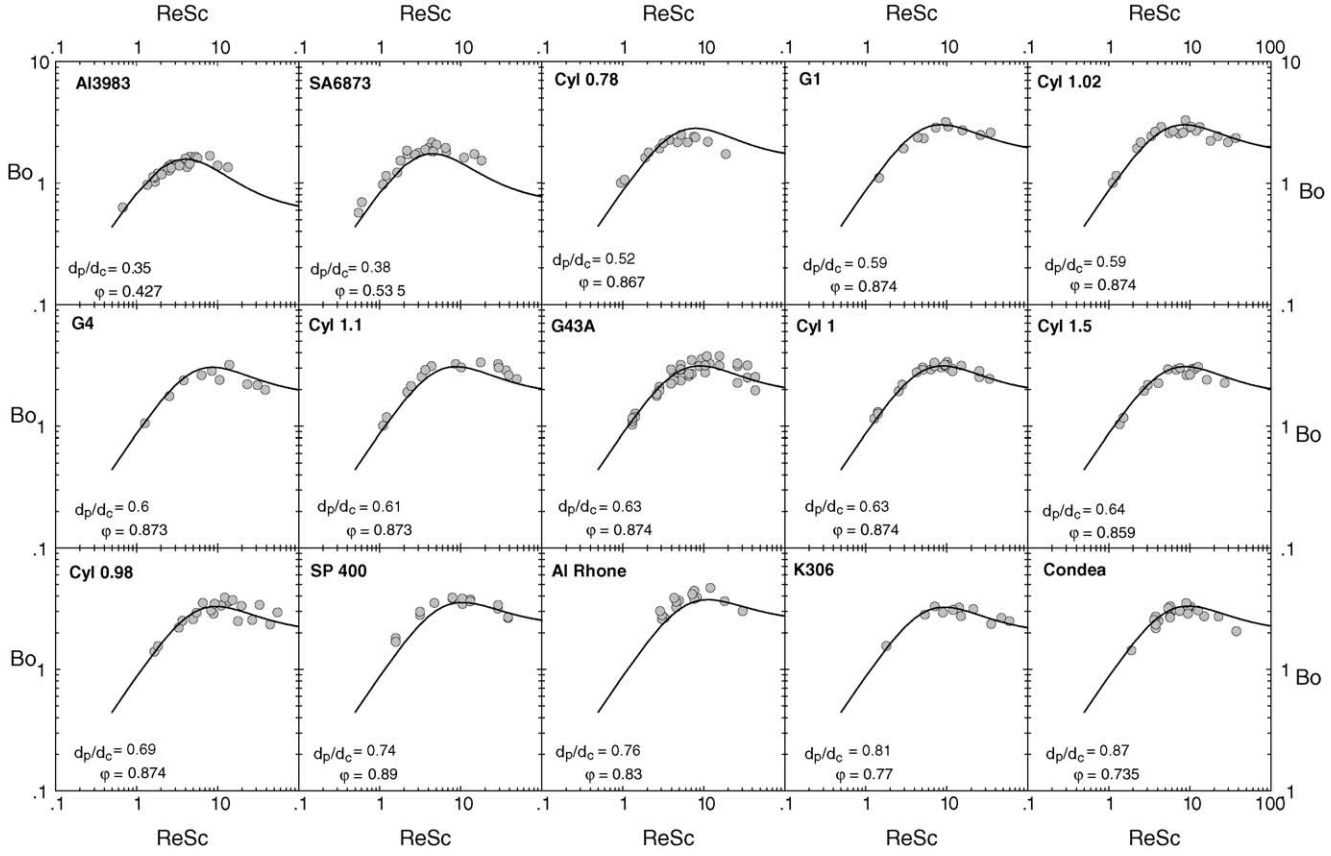

Fig. 6. *Bo–Re Sc* dependences for all studied pellets (6 types of non-porous cylindrical pellets, 9 types of non-spherical porous pellets with pores blocked by Porofil). Points: experimental; lines: calculated (Eq. (3) with parameters from Table 5).

correlation for non-porous pellets [16]:

$$\frac{1}{Bo} = \frac{\gamma}{Re\,Sc} + \frac{\lambda_0[1-\lambda_1(d_p/d_c)][1+\lambda_2(1-\varphi)]Re\,Sc}{\beta + Re\,Sc} \quad (3)$$

As can be seen from Fig. 6 the calculated *Bo* numbers are in the good agreement with SPSC experiments for a wide range of *Re Sc* ($Re\,Sc \in (0.6, 50)$), d_p/d_c ($d_p/d_c \in (0.35, 0.87)$) and φ ($\varphi \in (0.42, 0.89)$). Table 5 also contains parameters (γ, β, λ_0, λ_1) obtained only for spherical pellets for which $\varphi = 1$; this simplifies Eq. (3) to the following form (data for spherical pellets were already reported [16]):

$$\frac{1}{Bo} = \frac{\gamma}{Re\,Sc} + \frac{\lambda_0[1-\lambda_1(d_p/d_c)]Re\,Sc}{\beta + Re\,Sc} \quad (4)$$

Eq. (4) was verified for $d_p/d_c \in (0.56, 0.8)$. For spheres with diameters approaching the column diameter problems arise during recording of SPSC responses; the reason is probably the more complicated hydrodynamics of gas flow through the very narrow gap between packing and inner column wall.

Use of two variants of the *Bo–Re Sc* interpolation equation (Eq. (4) for spherical pellets and Eq. (3) for non-spherical pellets) reduces the standard errors of obtained parameters by about 50%.

As was shown previously [16], all dependences *Bo–Re Sc* pass through a maximum at $Re\,Sc_{opt}$. For the corresponding carrier-gas velocity the axial dispersion coefficient, E_{TC}, is the lowest. Hence, carrier-gas velocities around $Re\,Sc_{opt}$ are best suited for determination of effective diffusion coefficients, D_{TC}, through evaluation of responses of SPSC packed with porous pellets.

5. Conclusions

It was verified that it is possible to block pores in porous pellets by filling them with a liquid, possessing low viscosity and low vapour pressure. In this way the pore-diffusion steps in SPSC columns are eliminated; which permits reproducible determination of axial dispersion effects and overcomes mutual correlation of axial dispersion and pore-diffusion parameters.

Intrusion of extra-column effects into SPSC column responses was removed by the use of convolution of column responses for two column lengths. This allowed determination of axial dispersion characteristics with higher confidence.

Parameters of interpolation equations and (4) are based on pellets with different shapes, including also shapes recently introduced into chemical industry praxis. The use of two equations (one for spherical and another for non-spherical pellets) permits more accurate prediction of axial dispersion. For spherical pellets Eq. is based on data with pellet/column diameter ratios $d_p/d_c \in (0.56, 0.8)$. Parameters of Eq. (3) cover the intervals $d_p/d_c \in (0.35, 0.87)$ and $\varphi \in (0.42, 0.89)$. In all cases the *Re Sc* varied between 0.6 and 50.

Use of the obtained correlations for axial dispersion in the SPSC arrangement will improve significantly the confidence of pore-diffusion characteristic evaluated from responses of *SPSC packed with porous pellets of unusual shapes*. Pellets of these shapes show now growing practical importance and it is very difficult to obtain for them effective diffusion coefficient and/or transport characteristics by other experimental procedures.

Acknowledgement

The financial support of Grant Agency of the Czech Academy of Sciences (#A 4072404) and Grant Agency of the Czech Republic (104/04/0963, 203/03/H140) is gratefully acknowledged.

List of symbols

Bo	Bodenstein number ($=vd_p/E_{TC}$)
$c(t)$	tracer response of column II (length L_{II})
C	carrier-gas
d_c	internal column diameter
d_p	equivalent sphere diameter
D	diameter of cylindrical pellet
D_{TC}	effective pore-diffusion coefficient of the pair *T–C*
$\mathbf{D}_{TC}$	binary bulk-diffusion coefficient of the pair *T–C*
E_{TC}	axial dispersion coefficient of the pair *T–C*
$g(t)$	tracer response from column I (length L_I)
$h(t)$	tracer impulse response from column with length L_c
H	height of cylindrical pellets
L_c	$L_{II} - L_I$
L_I, L_{II}	lengths of columns ($L_{II} > L_I$)
Pe	Peclet number ($=vL_c/E_{TC}$)
Re	Reynolds number ($=vd_p\rho_C/\mu_C$)
Re Sc	$vd_p/\mathbf{D}_{TC}$
Sc	Schmidt number ($=\mu_C/\rho_C\mathbf{D}_{TC}$)
t	time
t_c	tracer-gas residence time ($=L_c/v$)
T	tracer-gas
v	carrier-gas interstitial linear velocity

Greek symbols

α	column void fraction
β, γ, λ_0, λ_1, λ_2	parameters (Eq. (3))
δ	diffusion term (Eq. (1))
ε	pellet porosity
μ_C	carrier-gas viscosity
ρ_C	carrier-gas density
φ	pellet sphericity

References

[1] P. Čapek, A. Seidel-Morgenstern, Appl. Catal. A: Gen. 211 (2001) 227.
[2] J. Haugaard, H. Livbjerg, Chem. Eng. Sci. 53 (1998) 2941.
[3] F.J. Keil, Catal. Today 53 (1999) 245.

[4] T.A. Nijhuis, L.J.P. van de Broeke, M.J.G. Linders, J.M. van de Graaf, F. Kapteijn, M. Makkee, J.A. Moulijn, Chem. Eng. Sci. 54 (1999) 4423.
[5] P. Schneider, J.M. Smith, AIChE J. 14 (5) (1968) 762.
[6] H.W. Haynes, Catal. Rev.-Sci. Eng. 30 (4) (1988) 563.
[7] D.S. Scott, W. Lee, J. Papa, Chem. Eng. Sci. 29 (1974) 2155.
[8] T. Li, Y. Zhu, S. Li, J. Zhu, B. Zhu, J. East China Univ. Sci. Technol. 26 (3) (2000) 256–259.
[9] C.A.V. Costa, A.E. Rodrigues, Ind. Eng. Chem. Res. 33 (1994) 1380–1390.
[10] J. Li, Y. Pan, M. Chen, B. Zhu, Fuel Sci. Technol. Int. 13 (7) (1995) 857–879.
[11] A.H.J. Colaris, J.H.B.J. Hoebink, M.H.J.M. de Croon, J.C. Schouten, AIChE J. 48 (11) (2002) 2587–2596.
[12] G. Yu, J. Yu, Z. Yu, Chem. Eng. J. 78 (2000) 141–146.
[13] M. Kubín, Collect. Czech. Chem. Commun. 30 (1965) 1104.
[14] E. Kučera, J. Chromatogr. 19 (1965) 237.
[15] O. Šolcová, P. Schneider, Collect. Czech. Chem. Commun. 61 (1996) 844.
[16] O. Šolcová, P. Schneider, Chem. Eng. Sci. 59 (6) (2004) 1301.
[17] M.F. Edwards, J.F. Richardson, Can. J. Chem. Eng. 48 (1970) 466.
[18] D.M. Himmelblau, K.B. Bischoff, Process Anal. Simul., Wiley, New York, 1968.
[19] W.H. Press, B.P. Flannery, S.A. Teukolsky, W.T. Vetterling, Numerical Recipes, Cambridge University Press, Cambridge, 1995.
[20] J. Valuš, P. Schneider, Appl. Catal. A: Gen. 16 (1985) 329.
[21] E.N. Fuller, P.D. Schettler, J.C. Giddings, Ind. Eng. Chem. 58 (5) (1966) 18.